Supplement of Atmos. Chem. Phys., 20, 13303–13318, 2020
https://doi.org/10.5194/acp-20-13303-2020-supplement

Atmospheric Chemistry and Physics
Open Access
EGU

Supplement of

Differences in the composition of organic aerosols between winter and summer in Beijing: a study by direct-infusion ultrahigh-resolution mass spectrometry

Sarah S. Steimer et al.

Correspondence to: Sarah S. Steimer (sarah.steimer@aces.su.se)

Table S1: final sample volume calculations, starred values indicate filters with low mass loadings, where two punches were used to obtain the extract.

Data set	Sample code	Date	Mass per Punch [µg]	Final volume [µl]	Final Concentration [$\mu g \cdot \mu l^{-1}$]
Winter High	026	03/12/2016	1584.5	1800	0.88
Winter High	019	26/11/2016	1371.1	1500	0.91
Winter High	018	25/11/2016	1214.6	1300	0.93
Winter High	002	09/11/2016	1186.0	1000	1.19
Winter High	027	04/12/2016	850.7	1000	0.85
Winter Low	028	05/12/2016	130.3	150	0.87
Winter Low	016	23/11/2016	101.5	120	0.85
Winter Low	007	14/11/2016	75.3*	180	0.84
Winter Low	015	22/11/2016	66.9*	120	1.11
Winter Low	014	21/11/2016	60.3*	120	1.00
Summer High	007	27/05/2017	546.3	450	1.21
Summer High	029	17/06/2017	471.7	450	1.05
Summer High	010	30/05/2017	321.0	270	1.19
Summer High	017	06/06/2017	311.9	270	1.16
Summer High	028	16/06/2017	290.7	270	1.08
Summer Low	012	01/06/2017	116.2*	200	1.16
Summer Low	020	08/06/2017	113.7*	200	1.14
Summer Low	003	23/05/2017	104.7*	200	1.05
Summer Low	035	23/06/2017	88.3*	150	1.18
Summer Low	004	24/05/2017	84.2*	150	1.12

Table S2: Gas pollutants and meteorological parameters for the individual filters and the composite samples. Temperature and relative humidity were measured on the IAP tower at 8 m height. Information regarding the acquisition of the gas-phase data can be found in Shi et al. (2019) and Squires et al. (2020).

Sample	O_3 [ppb]	CO [ppb]	NO [ppb]	NO_2 [ppb]	NO_y [ppb]	SO_2 [ppb]	RH [%]	T [°C]
WH	6.4	1926.0	61.9	49.2	120.5	7.9	59.7	5.4
WL	13.2	1141.1	18.0	25.3	49.4	3.6	29.4	1.8
SH	63.4	501.1	2.5	21.0	31.5	2.6	46.6	29.1
SL	38.8	457.8	7.3	20.6	34.7	0.8	49.8	25.7

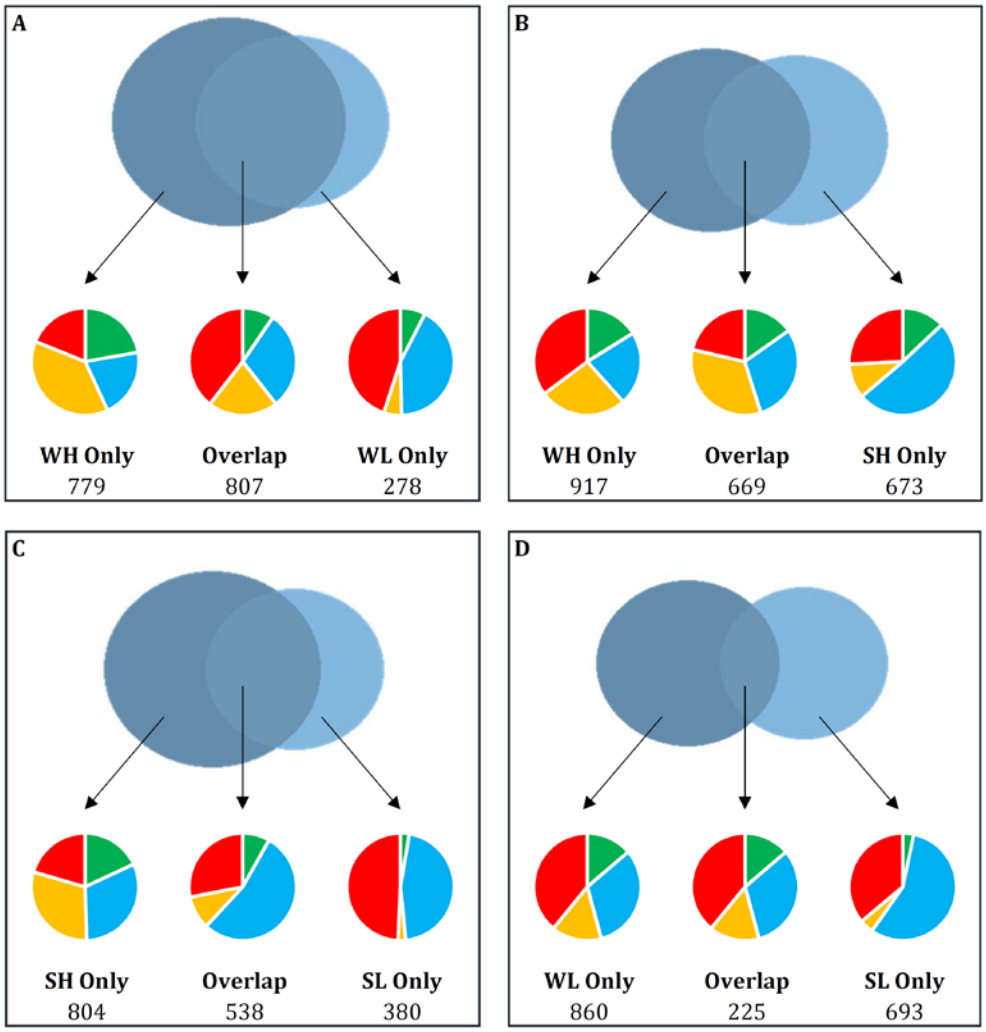

Figure S1: Venn diagrams illustrasting how many molecular formulas the various samples have in common. The Pie charts indicate the relative distribution of compound groups CHO (red), CHON (blue), CHOS (yellow) and CHONS (green) present in each section of the venn diagram, while the numbers below indicate the absolute numbers of different assigned formulas.

Signal intensities in the low mass loading samples were generally lower despite the attempt to have similar concentrations of total organic carbon in all samples. If sulphur-containing compounds are generally close to the detection limit, this could lead to them being not detected in the low mass loading samples despite having similar concentrations. To ensure that that is not the case, each sample set was separated by intensity of the peaks in the mass spectrum and the number of peaks were counted. The number of peaks in the high pollution sample for each season was subtracted from that in the low pollution sample, then divided by the high pollution sample to give an indication of the fractional loss or gain. The findings, displayed in Table S2, show that a considerable proportion of both lower and higher intensity peaks for CHOS and CHONS decreased from WH to WL and from SH to SL. This gives evidence to suggest that it is not just an artefact of the measurement technique, but it is in fact representative of changes in the chemical composition of the samples collected.

Table S3: percentage change of different compound and intensity groupings from high to low pollution conditions for both winter and summer relative to the high pollution sample. For scale, Table S2B shows the high pollution samples from which the relative values were obtained.

A	100x(WL-WH)/WH				100x(SL-SH)/SH			
Intensity Group	**CHO**	**CHON**	**CHOS**	**CHONS**	**CHO**	**CHON**	**CHOS**	**CHONS**
1,000,000-10,000,000	100	40	N/A	N/A	100	0	-100	N/A
100,000-1,000,000	255	275	800	-67	4	63	-78	-14
50,000-100,000	148	250	17	300	-13	263	-80	-36
10,000-50,000	-4	81	-52	-26	15	-5	-81	-68
5000-10,000	3	-30	-81	-69	5	-23	-71	-94
1000-5000	-73	-57	-91	-88	-38	-68	-45	-91

B	WH				SH			
Intensity Group	**CHO**	**CHON**	**CHOS**	**CHONS**	**CHO**	**CHON**	**CHOS**	**CHONS**
1,000,000-10,000,000	1	5	0	0	5	1	4	0
100,000-1,000,000	11	8	2	3	52	8	45	7
50,000-100,000	21	6	23	2	48	8	44	11
10,000-50,000	229	73	230	68	157	310	170	113
5000-10,000	102	118	101	86	41	128	21	36
1000-5000	100	193	110	91	13	87	11	22

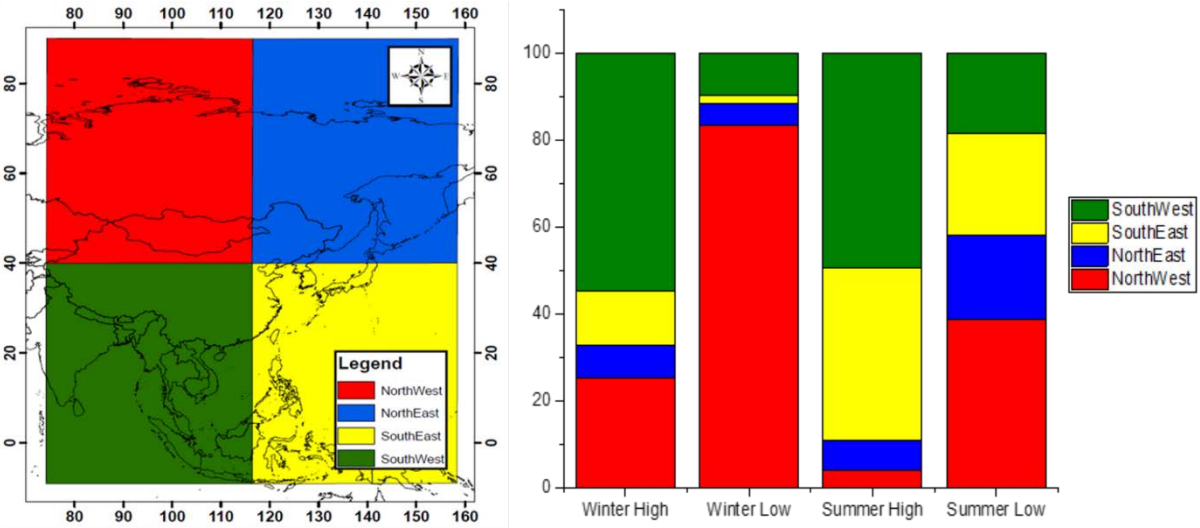

Figure S2: Percentage of time the air masses spent over specific regions for the different sampling condition. The centre of the map is located at the measurement site. Calculated via NAME model back trajectories.

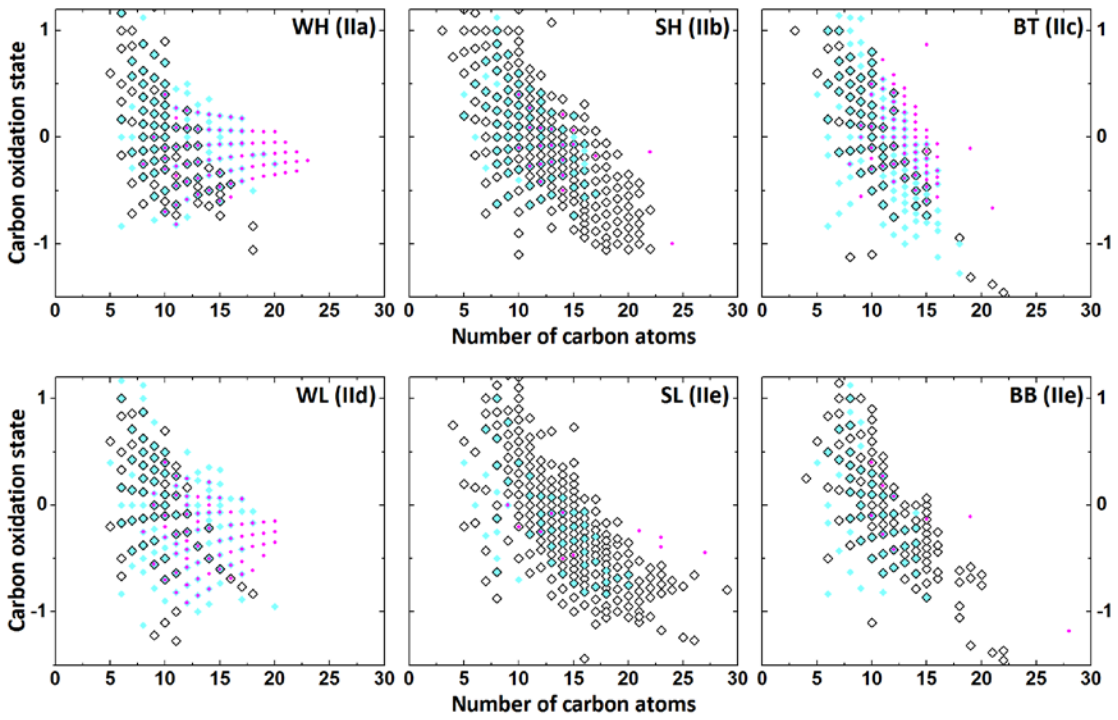

Figure S3: Plot of carbon oxidation state against carbon number for all CHON formulae in the WH, WL SH, SL, BT and BB samples. Polycyclic aromatic (2.7143 ≤ Xc), monocyclic aromatic (2.5000 ≤ Xc ≤ 2.7143) and non-aromatic (Xc ≤ 2.5000) formulae are depicted as magenta circles, cyan diamonds and open black diamonds respectively.

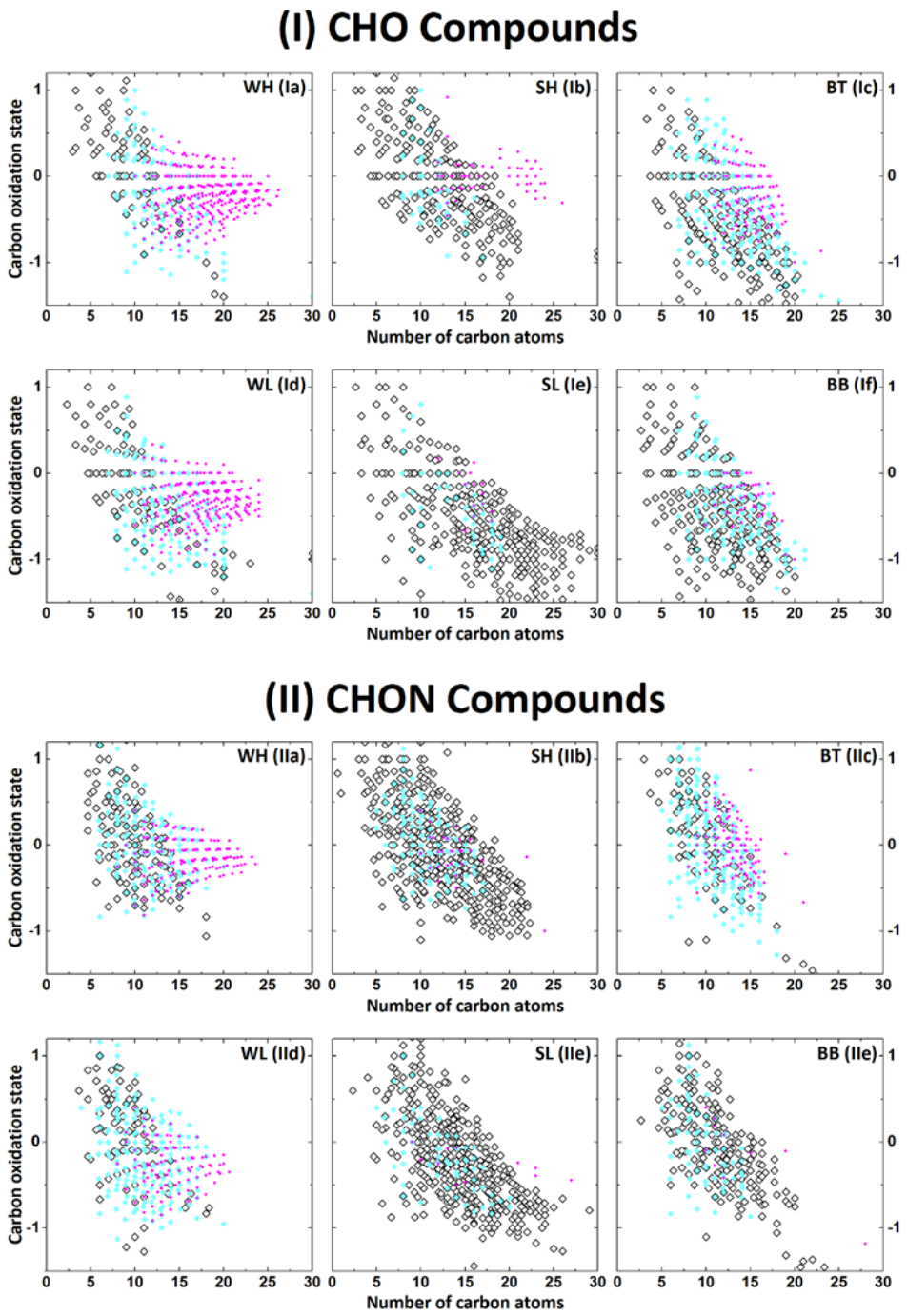

Figure S4: Plot of carbon oxidation state against carbon number for all CHO and CHON formulae in the WH, WL SH, SL, BT and BB samples. Polycyclic aromatic ($2.7143 \leq Xc$), monocyclic aromatic ($2.5000 \leq Xc \leq 2.7143$) and non-aromatic ($Xc \leq 2.5000$) formulae are depicted as magenta circles, cyan diamonds and open black diamonds respectively.

Table S4: Summary of statistics for the fits in Fig.8.

Plot	Pearson's r	Adjusted R^2	ANOVA: slope significantly different from 0?
a Winter CHOS/$SO4_4^{2-}$	0.82019	0.6318	yes
a Winter CHONS/$SO4_4^{2-}$	0.79535	0.5866	yes
b Summer CHOS/$SO4_4^{2-}$	0.52845	0.15914	no
b Summer CHONS/$SO4_4^{2-}$	0.40991	0.02936	no
c Winter CHON/NO_3^-	0.13094	-0.10571	no
c Winter CHONS/NO_3^-	0.83352	0.6566	yes
d Summer CHON/NO_3^-	-0.14193	-0.14317	no
d Summer CHONS/NO_3^-	0.63529	0.30419	no

References

Shi, Z., Vu, T., Kotthaus, S., Harrison, R. M., Grimmond, S., Yue, S., Zhu, T., Lee, J., Han, Y., Demuzere, M., Dunmore, R. E., Ren, L., Liu, D., Wang, Y., Wild, O., Allan, J., Acton, W. J., Barlow, J., Barratt, B., Beddows, D., Bloss, W. J., Calzolai, G., Carruthers, D., Carslaw, D. C., Chan, Q., Chatzidiakou, L., Chen, Y., Crilley, L., Coe, H., Dai, T., Doherty, R., Duan, F., Fu, P., Ge, B., Ge, M., Guan, D., Hamilton, J. F., He, K., Heal, M., Heard, D., Hewitt, C. N., Hollaway, M., Hu, M., Ji, D., Jiang, X., Jones, R., Kalberer, M., Kelly, F. J., Kramer, L., Langford, B., Lin, C., Lewis, A. C., Li, J., Li, W., Liu, H., Liu, J., Loh, M., Lu, K., Lucarelli, F., Mann, G., McFiggans, G., Miller, M. R., Mills, G., Monk, P., Nemitz, E., O'Connor, F., Ouyang, B., Palmer, P. I., Percival, C., Popoola, O., Reeves, C., Rickard, A. R., Shao, L., Shi, G., Spracklen, D., Stevenson, D., Sun, Y., Sun, Z., Tao, S., Tong, S., Wang, Q., Wang, W., Wang, X., Wang, X., Wang, Z., Wei, L., Whalley, L., Wu, X., Wu, Z., Xie, P., Yang, F., Zhang, Q., Zhang, Y., Zhang, Y. and Zheng, M.: Introduction to the special issue "In-depth study of air pollution sources and processes within Beijing and its surrounding region (APHH-Beijing)," Atmos. Chem. Phys., 19(11), 7519–7546, doi:10.5194/acp-19-7519-2019, 2019.

Squires, F. A., Nemitz, E., Langford, B., Wild, O., Drysdale, W. S., Acton, W. J. F., Fu, P., Grimmond, C. S. B., Hamilton, J. F., Hewitt, C. N., Hollaway, M., Kotthaus, S., Lee, J., Metzger, S., Pingintha-Durden, N., Shaw, M., Vaughan, A. R., Wang, X., Wu, R., Zhang, Q. and Zhang, Y.: Measurements of traffic dominated pollutant emissions in a Chinese megacity, Atmos. Chem. Phys. Discuss., 2020, 1–33, doi:10.5194/acp-2019-1105, in review, 2020.